Title	A shift in sphingolipid composition from C24 to C16 increases susceptibility to apoptosis in HeLa cells
Author(s)	Sassa, Takayuki; Suto, Shota; Okayasu, Yuriko et al.
Citation	Biochimica et Biophysica Acta (BBA): Molecular and Cell Biology of Lipids, 1821(7), 1031-1037 https://doi.org/10.1016/j.bbalip.2012.04.008
Issue Date	2012-07
Doc URL	https://hdl.handle.net/2115/49558
Type	journal article
File Information	BBA1821-7_1031-1037.pdf

A shift in sphingolipid composition from C24 to C16 increases susceptibility to apoptosis in HeLa cells

Takayuki Sassa[1], Shota Suto[1], Yuriko Okayasu, Akio Kihara*

Laboratory of Biochemistry, Faculty of Pharmaceutical Sciences, Hokkaido University, Sapporo, Japan

*Corresponding author

[1]These two authors contributed equally to this work

Address correspondence to:

Akio Kihara

Laboratory of Biochemistry

Faculty of Pharmaceutical Sciences, Hokkaido University

Kita 12-jo, Nishi 6-choume, Kita-ku, Sapporo 060-0812, Japan

Telephone: +81-11-706-3754

Fax: +81-11-706-4900

E-mail: kihara@pharm.hokudai.ac.jp

Abstract

Sphingolipids, major lipid components of the eukaryotic plasma membrane, have a variety of physiological functions and have been associated with many diseases. They have also been implicated in apoptosis. Sphingolipids are heterogeneous in their acyl chain length, with long-chain (C16) and very long-chain (C24) sphingolipids being predominant in most mammalian tissues. We demonstrate that knockdown of *ELOVL1* or *CERS2*, which catalyze synthesis of C24 acyl-CoAs and C24 ceramide, respectively, drastically reduced C24 sphingolipid levels with a complementary increase in C16 sphingolipids. Under *ELOVL1* or *CERS2* knockdown conditions, cisplatin-induced apoptosis significantly increased. Enhanced sensitivity to cisplatin-induced apoptosis exhibited close correlation with increases in caspase-3/7 activity. No significant alterations in sphingolipid metabolism such as ceramide generation were apparent with the cisplatin-induced apoptosis, and inhibitors of ceramide generation had no effect on the apoptosis. Apoptosis induced by UV radiation or C6 ceramides also increased in *ELOVL1* or *CERS2* knockdown cells. Changes in the composition of sphingolipid chain length may affect susceptibility to stimuli-induced apoptosis by affecting the properties of cell membranes, such as lipid microdomain/raft formation.

1. Introduction

Sphingolipids are major lipid constituents of eukaryotic plasma membranes and are indispensable for the growth and survival of organisms ranging from yeasts to mammals [1-3]. Mutations in genes involved in the metabolism of sphingolipids are associated with human diseases known as sphingolipidoses, which are characterized by the accumulation of particular sphingolipid subtypes [4]. Such mutations and the resulting sphingolipidoses provide evidence that sphingolipid homeostasis needs to be tightly coordinated.

In addition to their roles as cell membrane components, some sphingolipid metabolites act as signaling molecules [5, 6]. Ceramide, the backbone of sphingolipids, causes cell-cycle arrest and induces apoptosis [7, 8]. Ceramide is synthesized in the endoplasmic reticulum by a ceramide synthase (CERS) catalyzing an amide bond between a sphingoid base and a fatty acyl-CoA [6, 9]. Six mammalian CERSs (CERS1-6) have been identified. Each CERS exhibits characteristic substrate specificity toward fatty acyl-CoA(s) with particular acyl chain lengths and displays a cell type- or tissue-specific expression pattern [9, 10]. Thus, the relative expression levels of CERS isoforms partly account for the composition of ceramide and sphingolipid species with certain chain lengths within a cell or tissue.

Fatty acids in sphingolipids have acyl chains that vary in length from C16 to ≥C28. Fatty acids having a chain length of >20 are called very long-chain fatty acids (VLCFAs), and are produced from long-chain fatty acids (*e.g.*, palmitic acid (C16:0) or oleic acid (C18:1)), by elongation in the endoplasmic reticulum. In most mammalian tissues, the major sphingolipid species are C16:0 long-chain sphingolipids and C24 (C24:0 and C24:1) very long-chain sphingolipids. C24 sphingolipids are quite unique in that they contain C24 VLCFAs, which are almost exclusively utilized for C24 sphingolipids and not for

glycerolipid synthesis [11]. Enzymes involved in C24 sphingolipid generation include CERS2 and ELOVL1. CERS2, one of six mammalian CERS isoforms, is highly active toward C24 acyl-CoAs [12]. The C24 acyl-CoA utilized for C24 ceramide synthesis is a product of ELOVL1, one of seven mammalian elongases involved in the elongation of very long-chain acyl-CoAs [13]. Knockdown of *ELOVL1* or *CERS2* in HeLa cells significantly reduces the level of endogenous C24 sphingolipids [13]. Moreover, ELOVL1 forms a complex with CERS2, which also regulates its activity, so production of C24 acyl-CoA is coordinated with C24 sphingolipid synthesis [13].

In the plasma membrane, sphingolipids, together with cholesterol, form lipid microdomains, which are hypothesized to function as platforms for signal transduction [14, 15]. In neutrophil lipid microdomains, C24 lactosylceramides (but not C16 lactosylceramides) associate with and activate the acylated Src family kinase LYN [16]. We have shown in HeLa cells that *ELOVL1* knockdown impairs activation of LYN, suggesting that changes in the composition of sphingolipid chain length can affect the organization or function of the lipid microdomain [13, 16].

Apoptosis is a cellular process of cell death involved in a variety of developmental and pathological events [17, 18]. Sphingolipids, especially ceramides, have been implicated in apoptosis induced by stress stimuli including radiation, chemotherapeutic drugs, and tumor necrosis factor α [19]. To address the role of C24 sphingolipids in cellular functions, we examined the effect on apoptosis of a reduction in C24 sphingolipid levels in HeLa cells. We found that knockdown of *ELOVL1* or *CERS2* caused a reduction in C24 sphingolipids and a compensatory increase in C16 sphingolipids. This shift was accompanied by increased susceptibility of the cells to apoptosis induced by cisplatin, UV, or C6 ceramide. Results

obtained by experiments using tracers and pharmacological inhibitors suggest that cisplatin-induced apoptosis proceeded without alterations in sphingolipid metabolism, including ceramide generation. Taken together, these results suggest that the membrane environment formed by sphingolipids having specific chain lengths, rather than any increase or decrease in the amount of sphingolipids with a particular (polar) head group, such as ceramide, may affect the apoptosis signaling pathway.

2. Material and methods

2.1. Cell culture and transfection

HeLa cells were grown in DMEM D6046 (Sigma, St. Louis, MO) containing 10% fetal bovine serum and supplemented with 100 units/ml penicillin and 100 ⌈g/ml streptomycin. Transfections were performed using Lipofectamine Plus Reagent (Invitrogen, Carlsbad, CA) according to the manufacturer's instructions.

2.2. Plasmids

The pCE-puro 3xFLAG-1 vector and pCE-puro 3xFLAG-mElovl1 plasmid were described previously [13].

2.3. RNAi

The control siRNA and siRNAs for *CERS2* and *CERS4* were purchased from Qiagen and their use has been described previously [20]. The siRNA for *ELOVL1* was purchased from Sigma and its use has been described previously [13]. Four days prior to the experiments, HeLa cells (1.25 x 10^5 cells in 35 mm dish) were transfected with the appropriate siRNA using Lipofectamine RNAiMAX Reagent (Invitrogen).

2.4. RT-PCR

Total RNAs were extracted from HeLa cells using a NucleoSpin RNA II kit (Macherey-Nagel, Düren, Germany) according to the manufacturer's instructions. *ELOVL1*, *CERS2*, *CERS4* and *GAPDH* cDNAs were amplified from total RNAs by a SuperScript One-Step RT-PCR with

Platinum *Taq* kit (Invitrogen), following the manufacturer's instructions. Primers for

ELOVL1, *CERS2*, *CERS4* and *GAPDH* were described previously [13, 21].

2.5. Induction of apoptosis and its quantification by flow cytometry

Apoptosis in HeLa cells was induced by exposure to cisplatin (Sigma), C6 ceramide (Enzo

Life Sciences, Farmingdale, NY), or UV radiation. To induce apoptosis by cisplatin or C6

ceramide, cells were treated for 24 h with cisplatin or for 48 h with C6 ceramide. In some

experiments, myriocin (Sigma), FB_1 (Sigma), Z-VAD-FMK (R&D Systems, Minneapolis,

MN), or imipramine (Sigma) was added 24 h before cisplatin treatment or 20 h before C6

ceramide treatment. These inhibitors were present continuously until harvest. UV irradiation

was performed in a biological safety cabinet using a UV GL-15 lamp (Toshiba, Tokyo,

Japan). Prior to UV irradiation, culture medium was replaced with Opti-MEM I (Invitrogen),

and the dish tops were removed. Cells were treated for 10 sec with 2.2 $J/m^2/s$ UV-C light

(wavelength 253.7 nm). After the irradiation, cells were incubated in fresh culture medium

for 12 h. After trypsinization, the cells undergoing apoptosis were detected and quantified

using an Annexin V-FITC Apoptosis Detection Kit (Medical & Biological Laboratories,

Nagoya, Japan) and FACSCalibur flow cytometer (BD Biosciences, Franklin Lakes, NJ)

following the manufacturers' instructions.

2.6.Caspase-3/7 assay

Caspase-3/7 activities in cisplatin-treated HeLa cell extracts were quantified by a colorimetric

assay using an APOPCYTO Caspase-3 Colorimetric Assay Kit (Medical & Biological

Laboratories).

2.7. [³H]Sphingosine labeling assay

Labeling of cellular sphingolipids in HeLa cells using [³H]sphingosine, lipid extractions, and lipid separation by reverse-phase TLC were performed as described previously [13, 22]. Lipid separation by normal-phase TLC was performed using Silica Gel 60 HPTLC plates (Merck, Whitestation, NJ) with 1-butanol/acetic acid/ water (3:1:1, v/v).

2.8. Diacylglycerol kinase (DGK) assays

To quantify ceramide levels, DGK assays were performed as described previously [23].

3. Results

3.1. Increased susceptibility of HeLa cells to cisplatin-induced apoptosis following ELOVL1 knockdown

In HeLa cells, the amount of C24 ceramides is much higher than that of C16 ceramides, but knockdown of *ELOVL1* essentially reverses the composition so that there are almost no C24 ceramides and C16 ceramides are increased [13]. We treated control or *ELOVL1* siRNA-transfected cells with cisplatin, which is known to induce apoptosis through caspase activation [24], then compared the fractions of cells undergoing apoptosis. In the absence of cisplatin, the basal level of apoptosis in *ELOVL1* siRNA-transfected cells was comparable or slightly increased as compared with that of control siRNA-transfected cells (Figs. 1 and 6). Treatment with cisplatin, however, resulted in significantly more apoptosis in *ELOVL1* siRNA-transfected cells than in control siRNA-transfected cells (Fig. 1A). To confirm that the increase in cisplatin-induced apoptosis was due specifically to the *ELOVL1* knockdown and not to any off-target effect of the siRNA, we performed a rescue experiment by transfecting the cells with a mouse *Elovl1* expression plasmid. The nucleotide sequence of mouse *Elovl1* cDNA differs from that of the human sequence in the region targeted by the *ELOVL1* siRNA, so its expression should be resistant to the *ELOVL1* siRNA. As expected, introduction of mouse *Elovl1* into the *ELOVL1* siRNA-transfected cells significantly lowered the number of cells undergoing apoptosis (Fig. 1B).

3.2. ELOVL1 knockdown facilitates activation of caspase-3/7 in response to cisplatin treatment

To determine whether the increased cisplatin-induced apoptosis observed with *ELOVL1* knockdown is due to enhanced activation of apoptotic mediators, we monitored the protease activity of caspase-3/7 in control and *ELOVL1* siRNA-transfected cells. In the absence of cisplatin treatment, caspase-3/7 activity was nearly undetectable in control and *ELOVL1* knockdown cells (Fig. 2). Treatment with cisplatin dose-dependently increased caspase-3/7 activity in the control and *ELOVL1* knockdown cells, with the activation level significantly higher in the *ELOVL1* knockdown cells than in the control cells (Fig. 2). The increase in caspase-3/7 activity observed in the *ELOVL1* knockdown cells correlated well with the increased apoptosis (Figs. 1A and 2). These results suggest that changes in the composition of sphingolipid acyl chain length may affect the cellular membrane environment and thereby alter the signaling pathway leading to caspase-3/7 activation.

3.3. Increased susceptibility to cisplatin-induced apoptosis following CERS2 knockdown

In HeLa cells, CERS2, 4, and 5 are expressed, but C24 ceramides are predominantly synthesized by CERS2 [20]. *In vitro*, CERS4 exhibits similar substrate specificity to that of CERS2 [21]. To determine the contribution of CERS2 and CERS4 to C24 ceramide synthesis in HeLa cells, we knocked down *CERS2* or *CERS4* in these cells and examined lipid compositions. For comparison, *ELOVL1* knockdown was also performed. The knockdown efficiency of these siRNAs was confirmed by RT-PCR (Fig. 3A). We examined the composition of ceramide subspecies by labeling the cells with [^{3}H]sphingosine, followed by lipid extraction and separation using reverse-phase TLC. Knockdown of *CERS2* nearly eliminated C24:1 and C24:0 ceramides, but increased C16:0 ceramide (Fig. 3B). This effect was essentially identical to, or more severe than, the effect of *ELOVL1* knockdown (Fig. 3B).

Knockdown of *CERS4* resulted in subtle effects with decreases in C18:0 and C20:0 ceramides, and modest increases in C16:0 and C24:0 ceramides (Fig. 3B). Thus, CERS2 is the major ceramide synthase involved in the synthesis of C24 ceramides in HeLa cells. We next examined the effect of the changes in the sphingolipid chain length on cisplatin-induced apoptosis (Fig. 4). Knockdown of *CERS2* significantly increased apoptosis in response to cisplatin treatment as compared with control siRNA treatment (Fig. 4). Knockdown of *CERS4* had no effect, as was expected from the little change observed in the fatty acid composition of ceramides (Figs. 3B and 4).

3.4. Cisplatin-induced apoptosis in HeLa cells is not a characteristic ceramide-dependent apoptosis

The results above suggest that the fatty acid composition of sphingolipids affects apoptosis signaling. To identify the sphingolipid species involved in cisplatin-induced apoptosis, we first examined the effects of cisplatin treatment on sphingolipid metabolism using a [^{3}H]sphingosine labeling experiment. There were no obvious changes in the metabolism of sphingolipids such as ceramide, glucosylceramide, or sphingomyelin following treatment with 0.5, 1, 3, or 24 h cisplatin (Fig. 5A). Ceramides have been widely implicated in apoptosis [19], so we next examined the fatty acid compositions of ceramides by reverse-phase TLC. Cisplatin treatment did not result in any changes in the balance between long-chain ceramides and very long-chain ceramides, although a slight shift was observed in C24:0 ceramide to C22:0/C24:1 ceramide ratios (Fig. 5B). Treatment with the ceramide synthase inhibitor FB$_1$ resulted in dose-dependent inhibition of ceramide production, but no changes in fatty acid composition (Fig. 5B). A 24 h incubation with 20 μM FB$_1$

11

completely blocked ceramide synthesis (Fig. 5B and Supplementary Fig. 1A and B). FB_1

treatment also caused inhibition of the synthesis of downstream sphingolipids such as

sphingomyelin and glucosylceramide, but caused only slight increases in sphingosine and

sphingosine 1-phosphate (Supplementary Fig. 1A and B). Inhibition of ceramide synthesis

may cause accumulation of the ceramide synthase substrate sphingosine and its metabolite

sphingosine 1-phosphate.

To examine the involvement of ceramides in cisplatin-induced apoptosis in more

detail, we inhibited one of two pathways for ceramide generation, *de novo* synthesis (using

FB_1 or myriocin) or sphingomyelin hydrolysis (using imipramine). Myriocin is an inhibitor

of serine palmitoyltransferase, the enzyme catalyzing the first step of sphingolipid synthesis.

A [3H]palmitic acid labeling experiment in HeLa cells indicated that even 0.1 μM myriocin

effectively caused a reduction in sphingomyelin levels and a near absence of

glucosylceramide (Supplementary Fig. 2). Increasing the myriocin concentration had no

additional effect. Residual amounts of sphingomyelin did not disappear even at high levels

of myriocin, probably due to its production through the salvage pathway. Treatment with

myriocin or FB_1 did not affect the level of the cisplatin-induced apoptosis (Fig. 5C).

Imipramine, a potent inhibitor of acid sphingomyelinase that inhibits ceramide generated by

sphingomyelin hydrolysis, also had no significant effect on the apoptosis induced by

cisplatin (Fig. 5C). However, treatment with the broad caspase inhibitor Z-VAD-FMK

significantly inhibited the cisplatin-induced apoptosis, confirming that this cell death

mechanism depends on caspase activities [24].

Although apoptosis-dependent increases in ceramides have been reported in several

previous studies [19], no apparent increase in ceramide levels following cisplatin treatment

was observed in the [^{3}H]sphingosine labeling experiments (Fig. 5A and B and Supplementary Fig. 1B). Therefore, we measured the ceramide levels by DGK assay for confirmation. Again, no obvious difference in the levels of C16 or C24 ceramides between untreated and cisplatin-treated cells was found (Fig. 5D). These results suggest that cisplatin-induced apoptosis proceeds without alterations in sphingolipid metabolism including ceramide generation. Together with the knockdown analysis of individual CERS isoforms (Figs. 3 and 4), these data also suggest that in HeLa cells sphingolipids of specific acyl chain length may affect cisplatin-induced apoptosis, and that any increase or decrease in the amounts of sphingolipids having a particular (polar) head group, such as ceramide, may not be relevant.

3.5. Increased susceptibility to apoptosis induced by UV radiation or C6 ceramide following ELOVL1 or CERS2 knockdown

We next examined whether the observed increase in apoptosis accompanying the shift from C24 to C16 sphingolipids is specific to cisplatin or can be extended to other apoptosis-inducing stimuli. We treated *ELOVL1* or *CERS2* siRNA-treated HeLa cells with UV radiation or C6 ceramide, a cell-permeable short chain ceramide that can induce apoptosis in many cell types, including HeLa cells [25, 26] (Fig. 6). We found that, similar to the effect observed with cisplatin treatment, both UV radiation-induced and C6 ceramide-induced apoptosis were significantly enhanced in *ELOVL1* or *CERS2* siRNA-transfected cells compared with controls (Fig 6A and B). We examined the sensitivity of the C6 ceramide-induced apoptosis to inhibitors of ceramide generation, and found that neither FB$_1$ nor imipramine suppressed apoptosis (data not shown). These results suggest that

13

sphingolipids with specific acyl chain length may affect apoptosis in HeLa cells in response

to various stimuli, and this effect would seem to be ceramide-independent.

4. Discussion

Six CERS isoforms having different specificities for acyl chain length were recently identified [6, 9]. These studies revealed, at least in part, the basis of heterogeneity in mammalian sphingolipids, and suggested that sphingolipid species with specific acyl chain length may have unique cellular functions. Our finding, that changes in the cellular composition of sphingolipid acyl chain length affect sensitivity to cisplatin-induced apoptosis, supports this theory.

We succeeded in manipulating the chain length of cellular sphingolipid species in HeLa cells by knockdown of *ELOVL1* or *CERS2*. Cisplatin-, UV radiation-, and C6 ceramide-induced apoptosis were each significantly enhanced by knockdown of *ELOVL1* or *CERS2* (Figs. 1, 4 and 6). It remains to be determined whether changes in the composition of sphingolipid chain length affect apoptosis signaling directly or indirectly, as through a change in membrane properties such as lipid microdomain formation; we deem the latter to be more likely.

To reveal whether a specific sphingolipid is involved in the cisplatin-induced apoptosis, we examined sphingolipid metabolism using tracer experiments. Sphingolipid metabolism, including the levels and fatty acid composition of ceramides, which themselves have been widely implicated in apoptosis, was almost unchanged following cisplatin treatment (Fig. 5A and B). Furthermore, inhibitors of ceramide generation had no significant effect on apoptosis (Fig. 5C). These results suggest that ceramides may not play an important role in cisplatin-induced apoptosis of HeLa cells, at least under our experimental conditions, although we cannot exclude the possibility of their partial involvement. We did observe a compensatory increase in C16 sphingolipids upon *ELOVL1* or *CERS2* knockdown (Fig. 3B),

15

so we also cannot exclude the possibility that the reduction in C24 sphingolipids alters the levels of other lipids, and that these lipids may secondarily participate in regulating apoptosis signaling.

The pharmacological inhibitors myriocin, FB_1, and imipramine can affect the levels of certain sphingolipid species, but not their fatty acid compositions. In contrast, knockdown of *ELOVL1* or *CERS2* affects the fatty acid composition of sphingolipids. Considering that knockdown of *ELOVL1* or *CERS2* affected cisplatin-induced apoptosis whereas treatment with the inhibitors had no effect (Figs. 1, 4, and 5), we speculate that rather than any specific sphingolipid molecule being responsible, the membrane environment formed by the presence of sphingolipids having different acyl chain lengths (as described in detail below) affects apoptotic signals.

Glycosphingolipids and sphingomyelin exist in clusters and form lipid microdomains at the plasma membrane. Lipid microdomains play important roles in signal transduction at the membrane, as they provide a platform for many signaling molecules such as glycosylphosphatidylinositol-anchored proteins and acylated proteins [15, 27]. Several studies have characterized roles for sphingolipid acyl chain length in forming a membrane environment that includes domains such as lipid microdomains, which are platforms for signal transduction [16, 28]. Biophysical studies using artificial lipid bilayers have suggested that the extended portion of the C24 fatty acid moiety in C24 sphingolipids may cross the mid-plane of the lipid bilayer and interact with lipids in the opposing leaflet, thereby forming a partial interdigitation between the two leaflets [28]. Similarly, C24 lactosylceramides in the outer leaflet of the plasma membrane microdomain, but not C16 lactosylceramides, can cross the mid-plane of the lipid bilayer and interact with the acylated Src family kinase LYN in the

16

inner leaflet; this association promotes LYN activation [16]. *ELOVL1* knockdown in HeLa cells resulted in a failure of LYN activation [13], suggesting that there may be a signaling protein(s) with which C24 sphingolipids uniquely interact to regulate apoptosis. Interestingly, membrane vesicles prepared from livers or brains of *CerS2* knockout mice, which are severely deficient in C24 sphingolipids, exhibited increased membrane fluidity and altered morphology [29]. Treatment of HeLa cells with cisplatin induces cytochrome *c* release from mitochondria, leading to caspase-3/7 activation [24]. In cells with *ELOVL1* knockdown, enhanced cisplatin-induced apoptosis correlated with increased caspase-3/7 activity (Fig. 2). This suggests that changes in the composition of sphingolipid acyl chain length may affect the cellular membrane environment, and thereby alter the signaling pathway leading to caspase-3/7 activation. Sphingolipids are mainly present at the outer leaflet of the plasma membrane, so it is possible that sphingolipid chain length may affect anti-apoptotic/survival signaling regulated at the plasma membrane [30]. Alternatively, sphingolipids in mitochondria may affect mitochondrial outer membrane permeability, which regulates cytochrome *c* release in response to apoptosis signal, although the precise localization of sphingolipids in mitochondria has yet to be established [31]. *CerS2* knockout mice reportedly developed hepatocarcinomas; notably, increases in both apoptosis and proliferation of hepatocytes were observed [32, 33]. These increases accompanied changes in gene expression profiles and increases in the expression of cell-cycle regulators, including cyclin-dependent kinase inhibitor p21(WAF1/CIP1) and tumor suppressor p53 [33]. It is possible that the increased apoptosis in *ELOVL1* or *CERS2* knockdown HeLa cells may be caused by mechanisms similar to those observed in the livers of *CerS2* knockout mice.

Our results demonstrate that a shift from C24 to C16 sphingolipids affects apoptosis. Saturated C24 and C26 VLCFAs and sphingolipids that contain them are accumulated in X-linked adrenoleukodystrophy (X-ALD), which presents with symptoms of progressive demyelination and neurological dysfunction, as well as adrenal atrophy [34, 35]. ELOVL1 catalyzes the synthesis of C24:0- and C26:0-CoA in most cells, and knockdown of *ELOVL1* in fibroblasts derived from X-ALD patients significantly suppressed accumulation of C26:0 VLCFA [36]. Thus, C24 (and C26) sphingolipids may have multiple functions whose dysregulation could lead to pathological consequences. Future studies using genetically modified animals such as *Elovl1* knockout mice will be required to fully understand the physiological and pathological functions of C24 sphingolipids and saturated VLCFAs.

References

[1]   R.C. Dickson, C. Sumanasekera, R.L. Lester, Functions and metabolism of

sphingolipids in *Saccharomyces cerevisiae*, Prog. Lipid Res. 45 (2006) 447-465.

[2]   K. Hanada, Serine palmitoyltransferase, a key enzyme of sphingolipid metabolism,

Biochim. Biophys. Acta 1632 (2003) 16-30.

[3]   M.R. Hojjati, Z. Li, X.C. Jiang, Serine palmitoyl-CoA transferase (SPT) deficiency

and sphingolipid levels in mice, Biochim. Biophys. Acta 1737 (2005) 44-51.

[4]   F. Sabourdy, B. Kedjouar, S.C. Sorli, S. Colie, D. Milhas, Y. Salma, T. Levade,

Functions of sphingolipid metabolism in mammals — lessons from genetic defects,

Biochim. Biophys. Acta 1781 (2008) 145-183.

[5]   A. Kihara, S. Mitsutake, Y. Mizutani, Y. Igarashi, Metabolism and biological

functions of two phosphorylated sphingolipids, sphingosine 1-phosphate and

ceramide 1-phosphate, Prog. Lipid Res. 46 (2007) 126-144.

[6]   Y.A. Hannun, L.M. Obeid, Principles of bioactive lipid signalling: lessons from

sphingolipids, Nat. Rev. Mol. Cell Biol. 9 (2008) 139-150.

[7]   Y.A. Hannun, C. Luberto, Ceramide in the eukaryotic stress response, Trends Cell

Biol. 10 (2000) 73-80.

[8]   C. Luberto, J.M. Kraveka, Y.A. Hannun, Ceramide regulation of apoptosis versus

differentiation: a walk on a fine line. Lessons from neurobiology, Neurochem. Res.

27 (2002) 609-617.

[9]   Y. Mizutani, S. Mitsutake, K. Tsuji, A. Kihara, Y. Igarashi, Ceramide biosynthesis in

keratinocyte and its role in skin function, Biochimie 91 (2009) 784-790.

[10]   I. Becker, L. Wang-Eckhardt, A. Yaghootfam, V. Gieselmann, M. Eckhardt,

Differential expression of (dihydro)ceramide synthases in mouse brain:

oligodendrocyte-specific expression of CerS2/Lass2, Histochem. Cell Biol. 129

(2008) 233-241.

[11]   P.S. Sastry, Lipids of nervous tissue: composition and metabolism, Prog. Lipid Res.

24 (1985) 69-176.

[12]   E.L. Laviad, L. Albee, I. Pankova-Kholmyansky, S. Epstein, H. Park, A.H. Merrill,

Jr., A.H. Futerman, Characterization of ceramide synthase 2: tissue distribution,

substrate specificity, and inhibition by sphingosine 1-phosphate, J. Biol. Chem. 283

(2008) 5677-5684.

[13]   Y. Ohno, S. Suto, M. Yamanaka, Y. Mizutani, S. Mitsutake, Y. Igarashi, T. Sassa, A.

Kihara, ELOVL1 production of C24 acyl-CoAs is linked to C24 sphingolipid

synthesis, Proc. Natl. Acad. Sci. U. S. A. 107 (2010) 18439-18444.

[14]   D. Lingwood, K. Simons, Lipid rafts as a membrane-organizing principle, Science

327 (2010) 46-50.

[15]   K. Simons, E. Ikonen, Functional rafts in cell membranes, Nature 387 (1997)

569-572.

[16]   K. Iwabuchi, A. Prinetti, S. Sonnino, L. Mauri, T. Kobayashi, K. Ishii, N. Kaga, K.

Murayama, H. Kurihara, H. Nakayama, F. Yoshizaki, K. Takamori, H. Ogawa, I.

Nagaoka, Involvement of very long fatty acid-containing lactosylceramide in

lactosylceramide-mediated superoxide generation and migration in neutrophils,

Glycoconj. J. 25 (2008) 357-374.

[17]   T.G. Cotter, Apoptosis and cancer: the genesis of a research field, Nat. Rev. Cancer 9

(2009) 501-507.

[18]   P.M. Domingos, H. Steller, Pathways regulating apoptosis during patterning and

development, Curr. Opin. Genet. Dev. 17 (2007) 294-299.

[19]   B.J. Pettus, C.E. Chalfant, Y.A. Hannun, Ceramide in apoptosis: an overview and

current perspectives, Biochim. Biophys. Acta 1585 (2002) 114-125.

[20]   Y. Mizutani, A. Kihara, H. Chiba, H. Tojo, Y. Igarashi, 2-Hydroxy-ceramide

synthesis by ceramide synthase family: enzymatic basis for the preference of FA

chain length, J. Lipid Res. 49 (2008) 2356-2364.

[21]   Y. Mizutani, A. Kihara, Y. Igarashi, Mammalian Lass6 and its related family

members regulate synthesis of specific ceramides, Biochem. J. 390 (2005) 263-271.

[22]   A. Kihara, M. Ikeda, Y. Kariya, E.Y. Lee, Y.M. Lee, Y. Igarashi,

Sphingosine-1-phosphate lyase is involved in the differentiation of F9 embryonal

carcinoma cells to primitive endoderm, J. Biol. Chem. 278 (2003) 14578-14585.

[23]   Y. Kariya, A. Kihara, M. Ikeda, F. Kikuchi, S. Nakamura, S. Hashimoto, C.H. Choi,

Y.M. Lee, Y. Igarashi, Products by the sphingosine kinase/sphingosine 1-phosphate

(S1P) lyase pathway but not S1P stimulate mitogenesis, Genes Cells 10 (2005)

605-615.

[24]   X. Wang, J.L. Martindale, N.J. Holbrook, Requirement for ERK activation in

cisplatin-induced apoptosis, J. Biol. Chem. 275 (2000) 39435-39443.

[25]   Q. Dai, J. Liu, J. Chen, D. Durrant, T.M. McIntyre, R.M. Lee, Mitochondrial

ceramide increases in UV-irradiated HeLa cells and is mainly derived from

hydrolysis of sphingomyelin, Oncogene 23 (2004) 3650-3658.

[26]   W. Hu, R. Xu, G. Zhang, J. Jin, Z.M. Szulc, J. Bielawski, Y.A. Hannun, L.M. Obeid,

C. Mao, Golgi fragmentation is associated with ceramide-induced cellular effects,

Mol. Biol. Cell 16 (2005) 1555-1567.

[27] K. Kasahara, Y. Sanai, Functional roles of glycosphingolipids in signal transduction via lipid rafts, Glycoconj. J 17 (2000) 153-162.

[28] M.R. Morrow, D. Singh, D. Lu, C.W. Grant, Glycosphingolipid fatty acid arrangement in phospholipid bilayers: cholesterol effects, Biophys. J. 68 (1995) 179-186.

[29] L.C. Silva, O. Ben David, Y. Pewzner-Jung, E.L. Laviad, J. Stiban, S. Bandyopadhyay, A.H. Merrill, Jr., M. Prieto, A.H. Futerman, Ablation of ceramide synthase 2 strongly affects biophysical properties of membranes, J. Lipid Res. 53 (2012) 430-436.

[30] S. Fulda, D. Vucic, Targeting IAP proteins for therapeutic intervention in cancer, Nat. Rev. Drug Discov. 11 (2012) 109-124.

[31] G. Kroemer, L. Galluzzi, C. Brenner, Mitochondrial membrane permeabilization in cell death, Physiol. Rev. 87 (2007) 99-163.

[32] S. Imgrund, D. Hartmann, H. Farwanah, M. Eckhardt, R. Sandhoff, J. Degen, V. Gieselmann, K. Sandhoff, K. Willecke, Adult ceramide synthase 2 (CERS2)-deficient mice exhibit myelin sheath defects, cerebellar degeneration, and hepatocarcinomas, J. Biol. Chem. 284 (2009) 33549-33560.

[33] Y. Pewzner-Jung, O. Brenner, S. Braun, E.L. Laviad, S. Ben-Dor, E. Feldmesser, S. Horn-Saban, D. Amann-Zalcenstein, C. Raanan, T. Berkutzki, R. Erez-Roman, O. Ben-David, M. Levy, D. Holzman, H. Park, A. Nyska, A.H. Merrill, Jr., A.H. Futerman, A critical role for ceramide synthase 2 in liver homeostasis: II. insights into molecular changes leading to hepatopathy, J. Biol. Chem. 285 (2010)

10911-10923.

[34]   S. Kemp, R. Wanders, Biochemical aspects of X-linked adrenoleukodystrophy,

        Brain Pathol. 20 (2010) 831-837.

[35]   H.W. Moser, J. Borel, Dietary management of X-linked adrenoleukodystrophy, Annu.

        Rev. Nutr. 15 (1995) 379-397.

[36]   R. Ofman, I.M. Dijkstra, C.W. van Roermund, N. Burger, M. Turkenburg, A. van

        Cruchten, C.E. van Engen, R.J. Wanders, S. Kemp, The role of ELOVL1 in very

        long-chain fatty acid homeostasis and X-linked adrenoleukodystrophy, EMBO Mol.

        Med. 2 (2010) 90-97.

Figure captions

Fig. 1.   Increased susceptibility of HeLa cells to cisplatin-induced apoptosis following *ELOVL1* knockdown. (A) Cells were transfected with control or *ELOVL1* siRNAs (16 nM), then 3 days later were treated for 24 h with the indicated concentrations of cisplatin. Values shown are the percentages of cells exhibiting an Annexin V-FITC signal above the threshold level, and represent the mean ± SD from three independent experiments. Statistically significant differences are indicated (**$p < 0.01$; *t* test). (B) Cells were transfected with control or *ELOVL1* siRNAs, then 2 days later were transfected with the pCE-puro 3xFLAG-Elovl1 plasmid encoding mouse Elovl1, or with the pCE-puro 3xFLAG-1 vector. One day later, cells were treated for 24 h with the indicated concentrations of cisplatin. Data were obtained and are presented as in (A). Statistically significant differences are indicated (*$p < 0.05$, **$p < 0.01$; *t* test). *mElovl1*, mouse *Elovl1*.

Fig. 2.   *ELOVL1* knockdown facilitates activation of caspase-3/7 in response to cisplatin treatment. Cells were transfected with control or *ELOVL1* siRNA (16 nM), then 3 days later were treated for 24 h with the indicated concentrations of cisplatin. Total cell lysates were prepared, then incubated for 1 h at 37 °C with the DEVD-*p*NA peptide, a synthetic caspase-3/7 substrate labeled with *p*-nitroanilide. Caspase-3/7 activity was determined as a measure of free *p*NA level by monitoring an absorbance at 405 nm using an absorption spectrophotometer. Values represent the mean ± SD from three independent experiments. Statistically significant differences are indicated (**$p < 0.01$; *t* test).

Fig. 3. Knockdown of *ELOVL1* or *CERS2* causes changes in the fatty acid composition of ceramides in HeLa cells. Cells were transfected with the indicated siRNAs (16 nM for control and *ELOVL1*, 2 nM for *CERS2*, and 4 nM for *CERS4*) 3 days prior to assays. (A) Total RNA was extracted from the transfected cells and subjected to RT-PCR using primers specific for *ELOVL1*, *CERS2*, *CERS4* or *GAPDH*. (B) Cells were labeled with 0.5 μCi [^{3}H]sphingosine for 2 h at 37 ℃. Lipids were extracted, separated by reverse-phase TLC, and detected by autoradiography as shown in the right panel. The left panel shows ceramide standards carrying an acyl chain of C16:0, C20:0, C24:0, or C24:1, which were separated in parallel with the lipids in the right panel and stained with a cupric acetate/phosphoric acid solution.

Fig. 4. Increased susceptibility to cisplatin-induced apoptosis following *CERS2* knockdown. Cells were transfected with the indicated siRNAs (4 nM for control, 2 nM for *CERS2* and 4 nM for *CERS4*), then 3 days later were treated for 24 h in the absence or presence of 20 μM cisplatin. Cells were stained with Annexin V-FITC and analyzed using a FACSCalibur flow cytometer. Values shown are the percentages of cells exhibiting Annexin V-FITC signal above the threshold level, and represent the mean ± SD from three independent experiments. Statistically significant differences are indicated (**p < 0.01; *t* test).

Fig. 5. Sphingolipid levels are unchanged by cisplatin treatment in HeLa cells. (A) Cells were incubated with 30 μM cisplatin for the indicated times, then were labeled with 0.5 μCi [^{3}H]sphingosine for 2 h at 37 ℃. Lipids were extracted, separated by normal-phase TLC, and

26

detected by autoradiography. Cer, ceramide; GlcCer, glucosylceramide; Sph, sphingosine; S1P, sphingosine 1-phosphate; SM, sphingomyelin. (B) Cells were incubated with the indicated concentrations of FB_1 for 1 h, then were incubated for an additional 24 h in the absence or presence of 30 μM cisplatin. Cells were labeled with 0.5 μCi [^{3}H]sphingosine for 2 h at 37 ℃. FB_1 and cisplatin were present continuously until harvest. Lipids were extracted, separated by reverse-phase TLC, and detected by autoradiography. (C) Cells were incubated for 24 h in the absence or presence of cisplatin (30 μM). Where indicated, cells were preincubated with myriocin (1 μM), FB_1 (20 μM), imipramine (20 μM), or Z-VAD-FMK (30 μM), 24 h prior to addition of cisplatin. The inhibitors were present continuously until harvest. Values show the percentages of cells exhibiting Annexin V-FITC signal above the threshold level, and represent the mean ± SD from three independent experiments. Statistically significant differences are indicated (**$p < 0.01$; t test). (D) Cells were incubated in the absence or presence of 20 μM cisplatin for 0 or 24 h. Lipids were extracted and subjected to a DGK assay, together with standard ceramides to quantify ceramide levels. Ceramides were converted to ceramide 1-phosphates (C1Ps) by incubating with DGK and 1 μCi [©-^{32}P]ATP, followed by separation by normal-phase TLC and detection using a BAS2500 image analyzer.

Fig. 6.　　Increased susceptibility to apoptosis induced by UV radiation or C6 ceramide following *ELOVL1* or *CERS2* knockdown. (A) Cells were transfected with the indicated siRNAs (16 nM for control, 16 nM for *ELOVL1*, and 2 nM for *CERS2*), then 3 days later were irradiated for 10 sec with 2.2 J/m^2/s UV-C. Twelve hours after UV radiation, cells were stained with Annexin V-FITC and analyzed using a FACSCalibur flow cytometer. Values

show the percentages of cells exhibiting an Annexin V-FITC signal above the threshold level, and represent the mean ± SD from three independent experiments. Statistically significant differences are indicated (**$p < 0.01$; t test). (B) Cells were transfected as above with the indicated siRNAs, then 2 days later were treated for 48 h with the indicated concentrations of C6 ceramide. Cells undergoing apoptosis were detected, quantified, and presented as above.

Supplementary information

A shift in sphingolipid composition from C24 to C16 increases susceptibility to apoptosis in HeLa cells

Takayuki Sassa, Shota Suto, Yuriko Okayasu, Akio Kihara

Supplementary Material and methods

[³H]Palmitic acid labeling assay

Cells grown in 6 well plate were labeled with 50 μCi [³H]palmitic acid (60 Ci/mmol; American Radiolabeled Chemicals, St. Louis, MO) for 4 h at 37 ºC. Cells were collected and suspended in 200 μl phosphate-buffered saline, then lipids were extracted by successive additions of a 3.75-fold volume of chloroform/methanol/HCl (100:200:1, v/v), a 1.25-fold volume of chloroform, and a 1.25-fold volume of 1% KCl, with mixing. Phases were separated by centrifugation, and the organic phase was recovered. Lipids (300 μl) were saponified by adding 180 μl of 0.5 M NaOH in methanol and incubating at 37 ºC for 1 h. Samples were then treated with 90 μl of 1 M HCl in methanol, 180 μl chloroform, and 600 μl H_2O, with mixing. Phases were separated by centrifugation, and the organic phase was recovered, dried, and suspended in chloroform/methanol (2:1, v/v). The labeled lipids were separated on Silica Gel 60 HPTLC plates (Merck, Whitestation, NJ) with 1-butanol/acetic acid/ water (3:1:1, v/v) and detected by autoradiography.
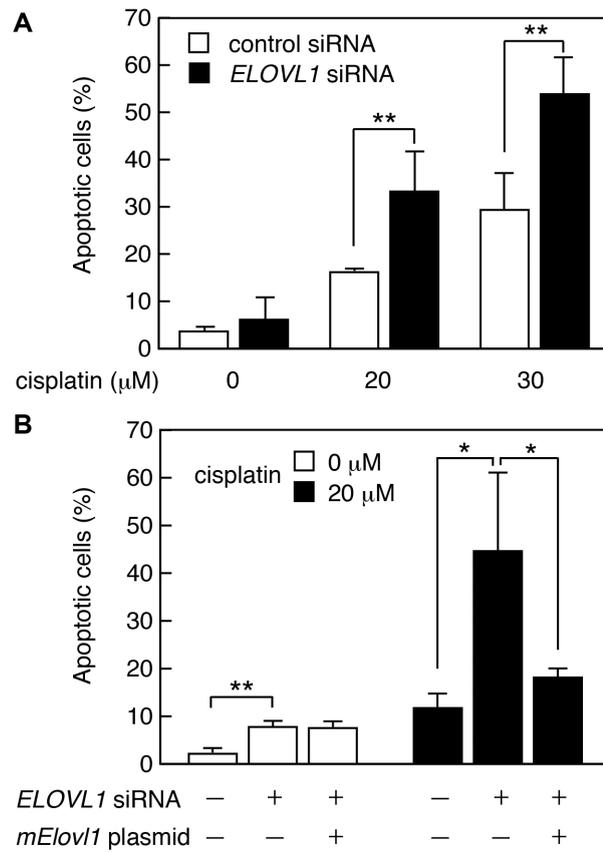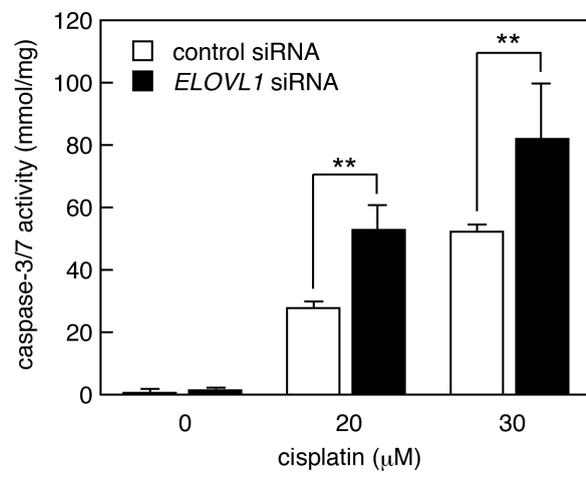
Supplementary Figure captions

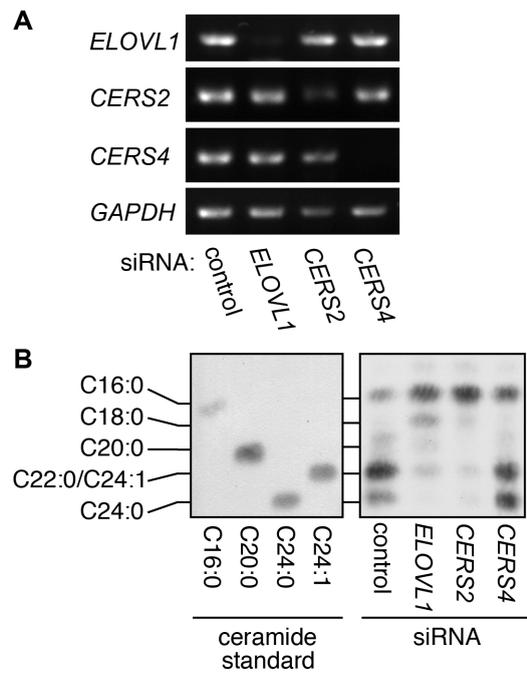**Supplementary Fig. 1.** Dose-dependent inhibition of sphingolipid synthesis by FB_1. (A) HeLa cells were incubated with the indicated concentrations of FB_1. After 1 h or 24 h incubation, cells were labeled with 0.5 μCi [^{3}H]sphingosine for 2 h at 37 °C. FB_1 was present continuously until harvest. Lipids were extracted, separated by normal-phase TLC, and detected by autoradiography. Cer, ceramide; GlcCer, glucosylceramide; Sph, sphingosine; S1P, sphingosine 1-phosphate; SM, sphingomyelin. (B) HeLa cells were incubated with the indicated concentrations of FB_1 for 1 h, then cells were incubated for an additional 24 h in the absence or presence of 30 μM cisplatin. Cells were then labeled with 0.5 μCi [^{3}H]sphingosine for 2 h at 37 °C. FB_1 and cisplatin were present continuously until harvest. Lipids were extracted, separated by normal-phase TLC, and detected by autoradiography.
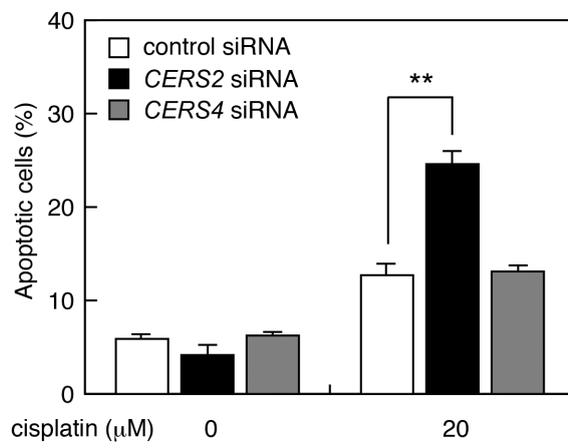
Supplementary Fig. 2. Myriocin inhibits *de novo* sphinogolipid synthesis in HeLa cells. Cells were treated with the indicated concentrations of myriocin for 1 h or 24 h. Cells were then labeled with 50 μCi [^{3}H]palmitic acid for 4 h at 37 °C. Myriocin was present continuously until harvest. Lipids were extracted, treated with 0.1 M NaOH (to hydrolyze the ester linkages in glycerolipids), separated by a normal-phase TLC, and detected by autoradiography. Pal, palmitic acid; GlcCer, glucosylceramide; SM, sphingomyelin.
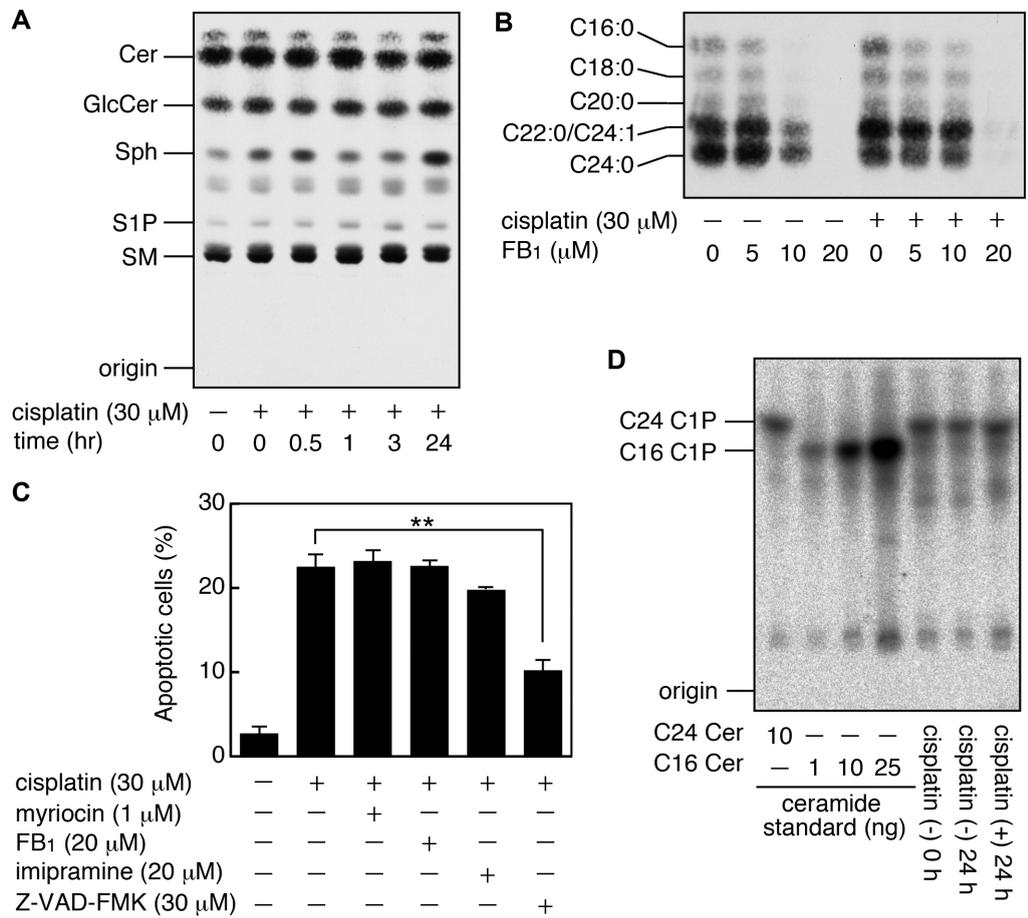
Sassa *et al.*, Figure 1
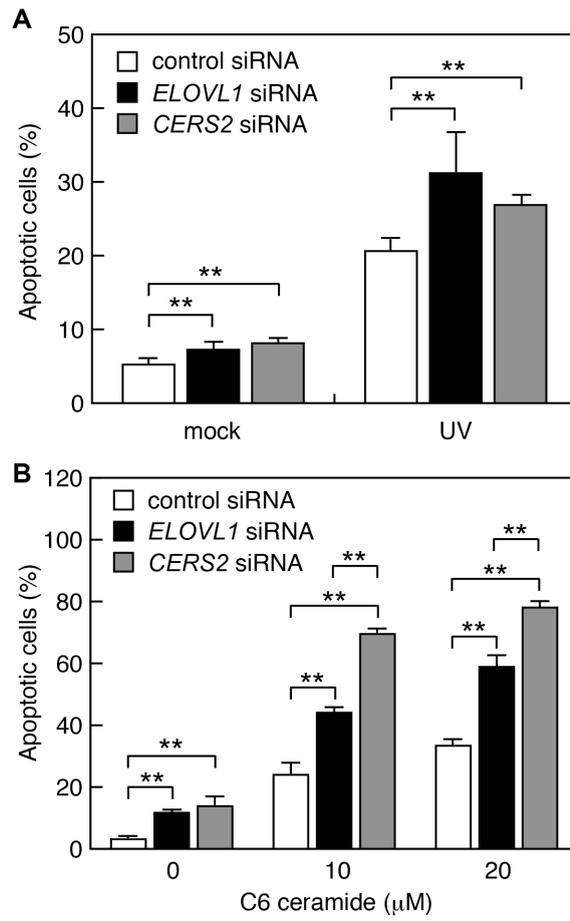
Sassa *et al.*, Figure 2

A

ELOVL1

CERS2

CERS4

GAPDH

siRNA: control ELOVL1 CERS2 CERS4

B

C16:0
C18:0
C20:0
C22:0/C24:1
C24:0

C16:0 C20:0 C24:0 C24:1 | control ELOVL1 CERS2 CERS4

ceramide standard | siRNA

Sassa *et al.*, Figure 3

Sassa *et al.*, Figure 4

A

Cer
GlcCer
Sph
S1P
SM

origin

| cisplatin (30 μM) | — | + | + | + | + | + |
| time (hr) | 0 | 0 | 0.5 | 1 | 3 | 24 |

B

C16:0
C18:0
C20:0
C22:0/C24:1
C24:0

| cisplatin (30 μM) | — | — | — | — | + | + | + | + |
| FB₁ (μM) | 0 | 5 | 10 | 20 | 0 | 5 | 10 | 20 |

C

Apoptotic cells (%)

cisplatin (30 μM)	—	+	+	+	+	+
myriocin (1 μM)	—	—	+	—	—	—
FB₁ (20 μM)	—	—	—	+	—	—
imipramine (20 μM)	—	—	—	—	+	—
Z-VAD-FMK (30 μM)	—	—	—	—	—	+

D

C24 C1P
C16 C1P

origin

| C24 Cer | 10 | — | — | — |
| C16 Cer | — | 1 | 10 | 25 |

ceramide standard (ng)

cisplatin (−) 0 h
cisplatin (−) 24 h
cisplatin (+) 24 h
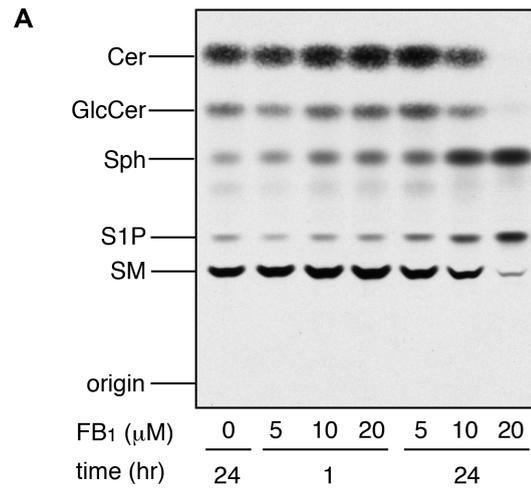
Sassa *et al.*, Figure 5

Sassa *et al.*, Supplementary Figure 1

Sassa *et al.*, Supplementary Figure 2